

Non-classical velocity statistics in a turbulent atomic Bose–Einstein condensate

Angela White,* Nick P. Proukakis, and Carlo F. Barenghi
*School of Mathematics and Statistics, Newcastle University,
Newcastle upon Tyne, NE1 7RU, England, UK.*

(Dated: August 10, 2018)

Abstract

In a recent experiment Paoletti *et al.* (Phys. Rev. Lett. **101**, 154501 (2008)) monitored the motion of tracer particles in turbulent superfluid helium and inferred that the velocity components do not obey the Gaussian statistics observed in ordinary turbulence. Motivated by their experiment, we create a small turbulent state in an atomic Bose-Einstein condensate, which enables us to compute directly the velocity field, and we find similar non-classical power-law tails. Our result thus suggests that non-Gaussian turbulent velocity statistics describe a fundamental property of quantum fluids. We also track the decay of the vortex tangle in the presence of the thermal cloud.

PACS numbers: 47.37.+q, 67.25.dk, 3.75.Lm, 03.75.Kk

*Electronic address: ang.c.white@gmail.com

Quantum turbulence (a dynamic tangle of discrete, reconnecting vortices) has been studied in superfluid ^4He [1], superfluid $^3\text{He-B}$ [2], and, more recently, in atomic Bose–Einstein condensates (BEC’s) [3, 4, 5]. The defining property of these quantum fluids is that the superfluid velocity field is proportional to the gradient of the phase of a complex order parameter, so the circulation is quantized in unit of the quantum κ (the ratio of Planck constant to the mass of the relevant boson). Therefore, whereas in classical ordinary fluids (such as air or water) the rotational motion is unconstrained, the velocity field around a quantum vortex decreases strictly as $\kappa/(2\pi r)$ where r is the distance away from the vortex axis.

Recent work has revealed that there are remarkable similarities between classical turbulence and quantum turbulence: the same Kolmogorov energy spectrum in continuously excited turbulence [6], the same temporal decay of the vorticity in decaying turbulence [7], the same pressure drops in pipe and channel flows [8], and the same drag crisis behind a sphere moving at high velocity [9]. These results have attracted attention to the problem of the relation between a classical fluid (which obeys the Euler or Navier–Stokes equations) and a quantum fluid [10], stimulating apparently simple questions such as whether classical behaviour is merely the consequence of many quanta. A recent experiment by Paoletti *et al.* [11] in superfluid ^4He has shed light onto this problem. Using a new visualization technique based on solid hydrogen tracers, Paoletti *et al.* found that the components of the turbulent velocity field do not obey the usual Gaussian distribution which is observed in ordinary turbulence [16], but rather follow power–law like behaviour.

The main aim of this Letter is to answer the question of whether non-Gaussian velocity statistics is a fundamental property of turbulence in a quantum fluid. To achieve this aim, we move from ^4He to an atomic BEC. The agreement that we find between these two distinct systems means that power–law behaviour is indeed typical of quantum fluids, in stark contrast with classical turbulence.

To create a vortex tangle in a harmonically confined atomic BEC we choose the technique of phase imprinting [13]. Although phase imprinting is not the only method which can be used to generate turbulence [5, 12], it is specific to BEC’s, and can in principle be exploited to non-destructively generate tangles engineered to be isotropic or polarized; this gives the technique its own numerical advantages over others. Having generated a vortex tangle, we also study its decay at zero temperature by evolving the three–dimensional (3D) Gross–

Pitaevskii equation for realistic experimental parameters, and also discuss the effect of the thermal cloud on this decay.

An ultra-cold dilute atomic gas confined in a spherical trap is described by the Gross–Pitaevskii equation (GPE) for the complex wavefunction Ψ . It is convenient to consider the GPE in dimensionless form as

$$i\frac{\partial}{\partial t}\psi = \left(-\frac{1}{2}\nabla^2 + \frac{1}{2}\mathbf{r}^2 + C|\psi|^2\right)\psi, \quad (1)$$

where \mathbf{r} is the position vector; $\psi = a_o^{3/2}N^{-1/2}\Psi$ is dimensionless and satisfies the constraint $\int d\mathbf{r}|\psi|^2 = 1$. In writing Eq. (1) we use the harmonic oscillator length $a_o = \sqrt{\hbar/(m\omega)}$ as the unit of distance and the inverse trapping frequency $1/\omega$ as the unit of time, where m is the mass of one atom, $C = 4\pi Na/a_o$ is the dimensionless measure of the interaction between bosons, N is the number of atoms and a is the scattering length.

Finite temperature effects can be simulated by replacing i at the L.H.S. of Eq. (1) with $(i-\gamma)$, where γ models the dissipation arising from the thermal cloud. Although such a model can be justified from first principles [14], one often resorts to the use of a (phenomenological) constant dissipation term [15] (as done here), as it is much less computationally intensive while still giving a qualitatively accurate prediction of the relevant physics.

We employ realistic experimental parameters for a ^{23}Na condensate ($a = 2.75$ nm) of $N = 10^5$ atoms and trapping frequency $\omega = 2\pi \times 150$ Hz, giving $C = 2.019 \times 10^3$, $a_o = 1.71$ μm and 1.06 ms as time unit. In a homogeneous condensate the healing length ξ is estimated by balancing the kinetic energy per particle and the interaction strength, which implies the (dimensionless) $\xi = (2Cn)^{-1/2}$ where $n = |\psi|^2$ is the condensate density. In a harmonic trap, n is position dependent, so we estimate the average ξ using the mean density; for example at $t = t_0$ (Fig. 1), $\langle n \rangle = 1.35 \times 10^{-3}$ and $\langle \xi \rangle = 0.43$.

Eq. (1) is evolved pseudo-spectrally via XMDS [17] in 3D using a 4th order Runge–Kutta method and periodic boundary conditions. The spatial domain $|x|, |y|, |z| \leq 8$ is discretised on a $128 \times 128 \times 128$ grid with timestep $\Delta t = 10^{-4}$. We have verified that the results are independent of spatial and temporal stepsize.

The initial condition is created by phase-imprinting a grid of 16 vortices oriented parallel to the Cartesian axes in a staggered way (no vortices intersect), and propagating this configuration for a short period in imaginary time (which is equivalent to substituting t with $-it$ in Eq. (1)) while continuously re-normalizing ψ , until the density adjusts to reveal

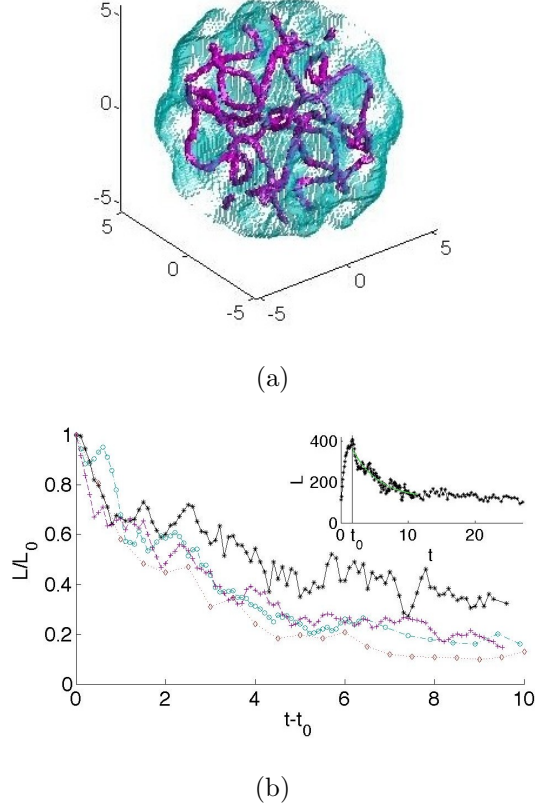


FIG. 1: (Color online) (a): Generated turbulent state within the condensate edge (blue shading), at $t_0 = 1.9$ and $\gamma = 0$; the maximum density (used to determine the condensate edge) is $n = 4.388 \times 10^{-3}$. (b) Evolution of normalized total length $L(t - t_0)/L_0$ for $\gamma = 0$ (black asterixes, $*$) 0.015 (purple pluses, $+$), 0.03 (blue circles, \circ) and 0.06 (red diamonds) corresponding to the same initial phase imprinting on a 128^3 grid; the inset also shows the initial increase of L for $t < t_0$ and the exponential fit for $\gamma = 0$ (solid green line).

the desired vortex structure. This is then propagated in real time. In the initial evolution period, the vortices reconnect and become excited, resulting in an increase in the total vortex line length L . This increase continues up to some time t_0 , when the $L(t)$ achieves its peak value L_0 , and a maximally tangled turbulent state has been generated (Fig. 1(a)). At this point the dimensionless vortex line density (vortex length divided by volume) is 0.79. The vortex line length evolution for $t > t_0$ is shown in Fig. 1(b). Since no energy is injected into the system the turbulence is not sustained but decays over a time scale of the order $t \approx 10$, as vortices further reconnect, break up and decay into sound waves [18], or leave the condensate. Our calculation lasts longer (up to $t = 27$) at which time one long vortex is left at the centre of the condensate and some shorter vortices, roughly aligned in the

same direction, surround it closer to the condensate's edge. Large volume oscillations of the condensate at 1/3 of the trap frequency are observed. Although the amplitude of these oscillations decreases as the turbulence decays, a method of exciting turbulence without inducing volume oscillations would be preferable for experiments.

At each time t we attribute a vortex core length to every point in the condensate at which the real and imaginary parts of ψ crosses zero (therefore defining the vortex axis) [19]. The total vortex length $L(t)$ is the sum of all identified vortex points within the condensate edge, which, throughout this work, is defined as the outermost points at which n drops below 25% of the maximum density. We find the decay of the vortex length is better fit by an exponential of the form $L(t - t_0)/L_0 \sim \exp(-c(t - t_0))$ (solid line in Fig. 1(b)), rather than $1/L(t - t_0) \propto t - t_0$ found in [1]. Fitting over 10 time units, yields consistent values for different grid sizes ($c = 0.151 \pm 0.005$ and 0.144 ± 0.007 for gridsizes of 128^3 and 256^3 respectively, with corresponding line lengths $L_0 = 406$ and 378). We have also checked that the decay of $L(t)$ is largely insensitive to the initial imprinted vortex configuration obtained by imprinting extra vortices.

To obtain a qualitative understanding of the effect of the thermal cloud, we have repeated the above calculation with dissipation parameters $\gamma = 0.015, 0.03$ and 0.06 . As anticipated, the role of temperature is to induce faster decay of the turbulent state, leading respectively to $c = 0.252 \pm 0.007, 0.274 \pm 0.006$ and 0.340 ± 0.018 (with corresponding $L_0 = 369, 339,$ and 300 , due to the damping in the initial period $t < t_0$).

Our next step is to analyse the turbulent (dimensionless) superfluid velocity field, which we compute directly from the definition $\mathbf{v}(\mathbf{r}) = (\psi^* \nabla \psi - \psi \nabla \psi^*) / (2i|\psi|^2)$. (the derivatives of ψ being obtained spectrally). The calculation is tested against the expected azimuthal velocity profile of a single vortex set along the z axis, which is $v_{\hat{\theta}} = \kappa / (2\pi r)$ where $\kappa = 2\pi$ is the quantum of circulation. Using the Madelung representation $\psi = \sqrt{n(\mathbf{r})} \exp[i\varphi(\mathbf{r})]$, yields $\mathbf{v}(\mathbf{r}) = \nabla\varphi(\mathbf{r})$, showing that the velocity depends only on the condensate phase φ .

We calculate the probability density function (PDF) of each Cartesian velocity component v_i ($i = x, y, z$) for $\gamma = 0$ and compare it to the form that a Gaussian PDF (gPDF) of the velocity would take:

$$\text{gPDF}(v_i) = \frac{1}{\sigma\sqrt{2\pi}} \exp\left(\frac{-(v_i - \tilde{\mu})^2}{2\sigma^2}\right), \quad (2)$$

where σ , σ^2 and $\tilde{\mu}$ are the standard deviation, variance and mean of the velocity distribution

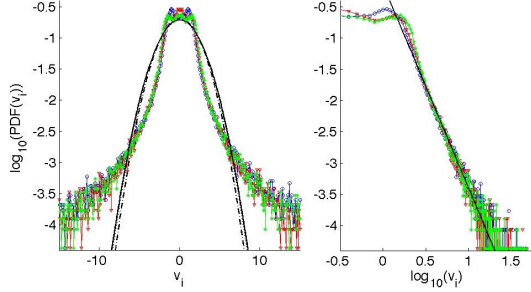


FIG. 2: (Color online) Left: 3D log-linear velocity PDFs corresponding to Fig. 1 ($\gamma = 0$): $\log_{10}[\text{PDF}(v_i)]$ vs. velocity component v_i , for v_x (blue circles, \circ), v_y (red triangles, ∇) and v_z (green asterixes, $*$), yielding following power law coefficients respectively $b = -3.27 \pm 0.04$, -3.54 ± 0.06 , -3.57 ± 0.06 . Corresponding $\log_{10}[\text{gPDF}(v_i)]$ plots shown by black dotted (\cdots , v_x), dash-dotted ($-$, v_y) and uniform ($-$, v_z) lines, which almost overlap. The velocity components are only sampled within the condensate edge (defined at 25% of the maximum density) thus excluding the outer region where the density drops to zero. Corresponding statistical values: $\sigma_i^2 = 4.1, 3.6, 4.2$ and $\tilde{\mu}_i = (4.6, 4.5, 4.6) \times 10^{-2}$. Right: Log-log plot of the same PDFs; the solid line is the power law fit to v_x .

(see Fig. 2). In evaluating the gPDF, we use the mean, standard deviation and variance of the actual velocity PDF. Power-law dependence of $\text{PDF}(v_i) \propto v_i^b$ is found from $\log(\text{PDF})$ vs $\log(v_i)$ plots of the positive velocity components, with $-3.57 < b < -3.27$ in all three directions.

It is apparent that our velocity statistics are non-Gaussian, consistently with the high velocity tails found experimentally by Paoletti *et al.* [11] in turbulent superfluid ^4He (their b is -3 , slightly less than ours). It is well-known that the PDF's of velocity components in ordinary turbulence are Gaussian [16]; our result thus supports the idea (put forward in Ref. [11]) that non-Gaussian velocity statistics are the unique signature of the quantized nature of the vortices.

We find that deviations from Gaussian behaviour are less pronounced (but still noticeable) if we omit sampling the velocity very near the axis when the density is less than a prescribed cutoff. Unlike a classical vortex, there are not individually distinguishable atoms which spin about the vortex axis, and the velocity field is entirely defined by the macroscopic phase $\varphi(\mathbf{r})$ irrespective of the density $n(\mathbf{r})$, so our procedure is justified. The small wiggles in the PDF for values close to zero may be a measure of the anisotropy of the vortex tangle in our

condensate and would not feature in velocity PDFs of a truly isotropic state of quantum turbulence in a larger condensate, or they could be due to the large volume oscillations of the 3D condensate.

The observed non-Gaussianity of the velocity statistics holds during the decay of the vortex tangle, suggesting that it is not necessarily caused by vortex reconnections, whose frequency depends on the vortex line density [20]. To verify that our result is general and does not depend on vortex line density or reconnections, we repeat the calculation in a two-dimensional (2D) BEC; such a condensate is created when the axial trapping frequency, ω_z , is much greater than the radial trapping frequency, ω_r , freezing out motion along z . The condensate in the radial plane is also described by Eq. (1), with $C \rightarrow C_{2d} = 2\sqrt{2\pi}aN/a_z$, and $\psi \rightarrow \psi_{2d} = a_r N^{-1/2} \Psi$ which relates the dimensionless wavefunction to the dimensional 2D condensate wavefunction, Ψ_{2d} , and $a_r = \sqrt{\hbar/(m\omega_r)}$ (here $a_z = \sqrt{\hbar/(m\omega_z)}$ are the harmonic oscillator lengths in the radial and z directions). To induce turbulence in a 2D BEC we imprint equal numbers of oppositely charged vortices randomly located and aligned along the axial direction [3]. Here we simulate a 2D ^{23}Na Bose gas with $N = 10^7$ atoms and condensate aspect ratio $\omega_z/\omega_r = 20$ (with $\omega_r = 7.5 \times 2\pi$ Hz), implying $C_{2d} = 8.06 \times 10^4$. The spatial computational domain $|x|, |y| \leq 25$ is discretized on a 1024×1024 grid with timestep $\Delta t = 10^{-4}$. Choosing our initial monitoring time arbitrarily at $t_0 = 4.4$, we have 86 vortices in the dimensionless condensate area 752, corresponding to a dimensionless vortex line density (number of vortices per unit area) of 0.11. We find a mean radial density $\langle n_{2d} \rangle = 1.23 \times 10^{-4}$, and an estimated healing length $\xi_{2d} = (2C_{2d}n_{2d})^{-1/2} = 0.225$. Proceeding as in 3D, the velocity PDF's and gPDF's of the 2D condensate are shown in Fig. 3 for $\gamma = 0$; we find again non-classical, non-Gaussian velocity statistics, with high velocity tails. This PDF lacks the small wiggles close to zero velocity observed in the 3D case, as the method of phase imprinting 42 positive and 42 negative vortices along the z axis in randomly selected locations across a much larger condensate generates a more isotropic turbulent state with negligible oscillations of the total radial area. As in 3D, we find a power-law correlation with velocity, $\text{PDF}(v_i) \propto v_i^b$ with -3.18 ± 0.08 for positive v_x and v_y velocity components respectively. Unlike the 3D case, vortex reconnections have played a negligible role in the state which is measured because during the measured timescale the number of vortices remains approximately the same as initially imprinted.

In conclusion, we have shown (under realistic experimental conditions) how phase

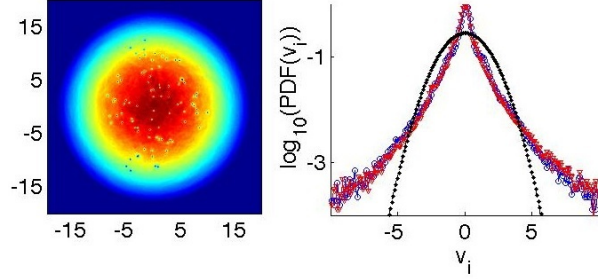


FIG. 3: Density (left) and velocity PDFs (right) for a 2D BEC at $t_0 = 4.4$ and $\gamma = 0$. The maximum density is $n = 2.057 \times 10^{-3}$. Left: 86 vortices (core radius ≈ 2.66) can be identified. Right: Plots of $\log_{10}[\text{PDF}(v_i)]$ and the corresponding $\log_{10}[\text{gPDF}(v_i)]$ vs v_i , where the v_x, v_y velocity components (sampled within the condensate edge) are given by blue circles (\circ) and red triangles (∇); corresponding gPDF's displayed by black dotted (\cdots) and dash-dotted ($-.$) lines. Statistical values: $\sigma_x^2 = \sigma_y^2 = 2.0$, $\tilde{\mu}_x = 5.8 \times 10^{-2}$, $\tilde{\mu}_y = 1.3 \times 10^{-2}$.

imprinting of a staggered array of straight non-intersecting vortices in a harmonically trapped ultra-cold atomic gas can be used to generate and study quantum turbulence in atomic BEC's. Finding velocity statistics similar to ^4He in these relatively small systems means that atomic BEC's can be used in the study of turbulence. We have also found that the decay of turbulence is faster in the presence of a thermal cloud, which we have modelled in a simple way.

Our main result is that the statistics of the turbulent superfluid velocity components are non-Gaussian, and exhibit power law tails similar to what has been recently found in an experiment with turbulent superfluid ^4He [11]. We confirmed our 3D result by repeating the calculation in a 2D condensate with a greater number of vortices, but lower dimensionless vortex line density, in a system in which vortex reconnections played virtually no role. Despite the huge difference in the ratio of intervortex spacing to vortex core radius in atomic BEC's (≈ 3 here) and in ^4He (10^5 to 10^6), we observed the same non-Gaussianity of the velocity, in contrast with the known Gaussianity of the velocity in classical turbulence. Our result thus suggests that power-law tails are a general feature of the constrained $1/r$ velocity fields which characterizes a quantum fluid.

The statistics of velocity components are thus macroscopic observables which distinguish between classical and quantum turbulence. It is worth remarking [21] that another such observable is the pressure spectrum, which, in 3D quantum turbulence, due to the $1/r$

velocity field and the singular nature of the vorticity, should obey a k^{-2} law (where k is the magnitude of the wavevector) rather than the $k^{-7/3}$ scaling which corresponds to the classical Kolmogorov $k^{-5/3}$ spectrum of the energy.

This research was supported by EPSRC grant EP/D040892/1 and by the Merit Allocation Scheme of the National Facility of the Australian Partnership for Advanced Computing.

-
- [1] Walmsley, P. M. and Golov, A. I., Phys. Rev. Lett. **100**, 245301 (2008).
 - [2] D. I. Bradley *et al.*, Phys. Rev. Lett. **101**, 065302 (2008); V. B. Eltsov *et al.*, Phys. Rev. Lett. **99**, 265301 (2007).
 - [3] T.L. Horng, C.H. Hsueh and S.C. Gou, Phys. Rev. A, **77**, 063625 (2008).
 - [4] K. Kasamatsu and M. Tsubota, in *Progress in Low Temperature Physics XVI*, ed. by W.P. Halperin and M. Tsubota, pg. 351, Elsevier (2009).
 - [5] E. A. Henn *et al.*, Phys. Rev. Lett. **103**, 045301 (2009).
 - [6] J. Maurer and P. Tabeling, Europhys. Lett. **43**, 29 (1998); C. Nore, M. Abid, and M.-E. Brachet, Phys. Rev. Lett. **78**, 3896 (1997); T. Araki, M. Tsubota, and S. K. Nemirovskii, Phys. Rev. Lett. **89**, 145301 (2002); M. Kobayashi and M. Tsubota, Phys. Rev. Lett. **94**, 065302 (2005).
 - [7] M. R. Smith *et al.*, Phys. Rev. Lett. **71**, 2583 (1993); C.F. Barenghi and L. Skrbek, J. Low Temp. Physics **146**, 5 (2007).
 - [8] P. L. Walstrom *et al.*, Cryogenics **28**, 101 (1998).
 - [9] M. R. Smith, D. K. Hilton, and S. V. Van Sciver, Phys. Fluids, **11**, 751 (1999).
 - [10] W. F. Vinen and J. J. Niemela, J. Low Temp. Phys. **128**, 167 (2002), and Erratum, **129**, 213 (2002); C.F. Barenghi, Physica D, **237**, 2195 (2008).
 - [11] M.S. Paoletti *et al.*, Phys. Rev. Lett. **101**, 154501 (2008).
 - [12] N.G. Berloff and B. Svistunov, Phys. Rev. A. **66**, 013603 (2002); N.G. Parker and C.S. Adams, Phys. Rev. Lett **95**, 145301 (2005); M. Kobayashi and M. Tsubota, Phys. Rev. A **76**, 045603 (2007); M. Kobayashi and M. Tsubota, J. Low. Temp. Phys. **150**, 587 (2008); E. A. Henn *et al.*, Phys. Rev. Lett. **103**, 045301 (2009).
 - [13] S. Burger *et al.*, Phys. Rev. Lett., **83**, 5198, 1999; A.E. Leanhardt *et al.*, Phys. Rev. Lett. **89**, 190403 (2002).

- [14] A.A. Penckwitt, R.J. Ballagh and C.W. Gardiner, Phys. Rev. Lett. **89**, 260402 (2002); N.P. Proukakis and B. Jackson, J. Phys. B **41**, 203002 (2008).
- [15] S. Choi, S.A. Morgan and K. Burnett, Phys. Rev. A. **57**, 4057 (1998); E.J.M. Madarassy and C.F. Barenghi, J. Low Temp. Physics **152**, 122 (2008); M. Tsubota *et al.*, Phys. Rev. A **65**, 023603 (2002).
- [16] A. Vincent and M. Meneguzzi, J. Fluids Mech. **225**, 1 (1991); A. Noullez *et al.*, J. Fluid Mech. **339**, 287 (1997); T. Gotoh *et al.*, Phys. of Fluids **14**, 1065 (2002).
- [17] Refer to <http://www.xmds.org> for a detailed description.
- [18] C.F. Barenghi *et al.*, J. Low Temp. Physics, **138**, 629 (2005); M. Leadbeater *et al.*, Phys. Rev. A **67**, 015601 (2002).
- [19] Peter Mason, Ph.D. Thesis, University of Cambridge (2009).
- [20] C.F. Barenghi and D.C. Samuels, J. Low Temp. Physics **36**, 281 (2004). M. Tsubota, T. Araki and S.K. Nemirowskii, Phys. Rev. B **62**, 11751 (2000).
- [21] D. Kivotides *et al.*, Phys. Rev. Lett. **87**, 275302 (2001).